ELECTRON STATES IN GaAs/$Ga_{1-x}Al_xAs$ HETEROSTRUCTURES: NONPARABOLICITY AND SPIN-SPLITTING*

F. Malcher, G. Lommer, U. Rössler
Institut für Theoretische Physik, Universität Regensburg,
D-8400 Regensburg, Federal Republic of Germany

(received 2/24/86 by G.H. Döhler, accepted 3/28/86)

We investigate the influence of the nonparabolicity of bulk bandstructure on the electron subbands in GaAs/$Ga_{1-x}Al_xAs$ heterojunctions. Our calculation is based on a self-consistent solution of the subband problem in the parabolic approximation and takes into account the nonparabolic contributions (of order k^3 and k^4) and the spin-orbit term $\sim(\underline{k}\times\underline{E})\cdot\underline{\sigma}$ by perturbation theory. The calculated electron subbands exhibit a nonparabolic dispersion and spin-splitting, whose variation with Al-concentration x and free carrier density N_s is investigated.

1. Introduction

The increasing amount of experimental work on electron subbands in GaAs/$Ga_{1-x}Al_xAs$ heterojunctions has more recently led to various theoretical investigations of these states. Ando,[1,2] Bastard,[3] Stern and DasSarma,[4] and Hurkx and van Haeringen[5] performed numerical or/and variational self-consistent calculations of the subband problem using an effective-mass Hamiltonian in the simplest, i.e. parabolic approximation for the kinetic energy. Earlier theoretical work is presented in the review article by Ando, Fowler, and Stern.[6] With the exception of Ref. 1, where nonparabolic corrections to the subband effective-mass have been estimated, the influence of the nonparabolicity of the bulk band structure on the subband states in GaAs/$Ga_{1-x}Al_xAs$ heterostructures is not considered in the above mentioned literature.

The nonparabolicity of the bulk band structure, originally understood as a small-gap effect, is usually described in Kane's model,[7] which takes into account the mixing between conduction (Γ_{6c}) and valence band ($\Gamma_{7v}+\Gamma_{8v}$) in a 8×8 matrix Hamiltonian. For large gap semiconductors this model is not appropriate, because the coupling between the lowest conduction band (Γ_{6c}) and the p-antibonding conduction band ($\Gamma_{7c}+\Gamma_{8c}$) becomes equally important and should be considered on equal footing. This leads to an extended Kane model for the bulk band structure in the vicinity of the Γ point,[8] which in addition takes into account the influence of more remote bands by second order perturbation theory. For an investigation of subbands in heterojunctions or quantum wells, including the nonparabolicity effects, this 14×14 matrix Hamiltonian ought to be considered as kinetic energy operator. This, however, would make the subband problem an awfully complex one. Lassnig[9] considered a simplified version of the extended Kane model, which does not include inversion-asymmetry induced terms and the coupling to remote bands. He reduced the set of 14 coupled equations by eliminating all but the conduction band envelope functions. By this reduction, which is analogous to Ohkawa and Uemura's[10] treatment of quantized surface states on a narrow-gap semiconductor, he obtained an effective-mass Hamiltonian acting in the twofold conduction band space.

In contrast our calculation is based on a reduction of the *bulk* Hamiltonian in the extended Kane model[8] to a 2×2 conduction band Hamiltonian by means of higher perturbation theory,[11] which contains terms of third and fourth order in the wave vector components. This Hamiltonian can also be obtained by an invariant expansion in the twofold space of the lowest conduction band states with the weighting factors taken from $\underline{k}\cdot\underline{p}$ theory.[11] In addition the invariant expansion yields as a cross-term between the $\underline{k}\cdot\underline{p}$ term and the coupling mediated by the interface electric field ($e\underline{E}\cdot\underline{r}$), the so-called spin-orbit term $\sim(\underline{k}\times\underline{E})\cdot\underline{\sigma}$, which is responsible for the spin-splitting of the subbands due to the symmetry breaking effect of the interface potential.[9,10,12] We use this 2×2 matrix Hamiltonian as effective-mass operator by replacing k_z (the wave vector component normal to the interface) by -id/dz and add the interface potential U(z) in the diagonal to obtain the subband Hamiltonian (Section 2). As the nonparabolic contributions and the spin-orbit term are only small corrections to the subband problem, we first perform a self-consistent numerical calculation in the parabolic approximation

*Work supported in part by the Deutsche Forschungsgemeinschaft

0749-6036/86/030267+06 $02.00/0

(Section 3) and then consider these corrections by perturbation theory (Section 4). We present results (subband energies, effective-masses and spin-splittings) for the two lowest subbands in $GaAs/Ga_{1-x}Al_xAs$ heterojunctions for $0.2 \le x \le 0.4$ and electron concentrations $10^{11}cm^{-2} \le N_s \le 1.2 \cdot 10^{12}cm^{-2}$ and calculate also the expectation value of the electric field for the lowest subband. It turns out that this expectation value differs from zero, in contrast to an earlier assumption made for subband states in a MIS inversion layer.[13] Preliminary results, including the effect of a magnetic field, have been published in Ref. 14.

2. The 2×2 Subband Hamiltonian

Following the concept of an invariant expansion[11,15] we construct the kinetic energy operator acting in the twofold space of the lowest conduction band states as a series of products of irreducible tensor components $K_L^{(\kappa,\lambda)*}(\underline{k},\underline{E})$ and a complete set of orthogonal 2×2 matrices $X_L^{(\kappa,\lambda)}$

$$H(\underline{k},\underline{E}) = \sum_{\kappa,\lambda} a_{\kappa\lambda} \sum_L X_L^{(\kappa,\lambda)} K_L^{(\kappa,\lambda)*}(\underline{k},\underline{E}) \quad (1)$$

The tensor components $K_L^{(\kappa,\lambda)*}(\underline{k},\underline{E})$ represent symmetrized products of the components of the electron wave vector $\underline{k}$ (up to fourth order) and the interface electric field $\underline{E}$, which transform according to the irreducible representations Γ_κ of the zinc-blende point group T_d and have the same time-reversal symmetry as the matrices $X_L^{(\kappa,\lambda)}$. For the basis matrices $X_L^{(\kappa,\lambda)}$ we choose $X_1^{(1)}=\mathbf{1}_2$ and $X_\alpha^{(4)}=\{\sigma_\alpha|\alpha=x,y,z\}$. The resulting terms are listed in Table 1.
$K_1^{(1,2)*}$ is the kinetic energy operator in the parabolic approximation. The terms $K_1^{(1,3)*}$ and $K_1^{(1,4)*}$ represent isotropic and anisotropic $\underline{k}$ nonparabolicity of the bulk conduction band. The remaining terms in Table 1 are the inversion-asymmetry induced $\underline{k}^3$ nonparabolicity and the spin-orbit term, which both contribute to a spin-splitting of the subband states for finite wave vector. The expansion coefficients $a_{\kappa\lambda}(\kappa=1,4)$ have been derived in Ref. 11 by reducing the original 14×14 Hamiltonian of the extended Kane model to a (2×2) Hamiltonian by higher order perturbation calculation. They can be expressed by momentum matrix elements and energy gaps, which are well known[16] for GaAs and AlAs and are obtained for $Ga_{1-x}Al_xAs$ by linear interpolation of the energy gaps. The weighting factor a_{64} can be determined from the results of a second order perturbation treatment of the $\underline{k}\cdot\underline{p}$ and $e\underline{E}\cdot\underline{r}$ couplings.[14] Numerical values for the expansion coefficients $a_{\kappa\lambda}$ are given in Table 2. It is important to note, that within our model the values of $a_{\kappa\lambda}$ change discontinuously at the interface. For comparison we give in Table 2 also some values of $a_{\kappa\lambda}$, when contributions from inversion-asymmetry induced terms and from remote bands are neglected as in previous work.[9]

The Hamiltonian for the subband problem is then obtained by replacing in $H(\underline{k},\underline{E})$ of Eq. 1 $\underline{k}$ by $-i\nabla$ and adding the interface potential $U(z)$ in the diagonal. In order to guarantee flux conservation across the interface, we must adopt the hermitian form of this Hamiltonian, thus the leading term of the kinetic energy operator appears as[17,18]

$$H_{kin} = -\frac{\hbar^2}{2} \nabla \frac{1}{m^*(z)} \nabla \quad (2)$$

The subband Hamiltonian then reads

$$H_{SB} = (H_{kin} + U(z))\mathbf{1}_2 + H_1 \quad (3)$$

where

$$H_1 = (a_{13}K_1^{(1,3)*} + a_{14}K_1^{(1,4)*})\mathbf{1}_2 + \sum_{\alpha=x,y,z}(a_{42}K_\alpha^{(4,2)*} + a_{64}K_\alpha^{(6,4)*})\sigma_\alpha \quad (4)$$

contains the nonparabolic terms and the spin-orbit coupling. In the following Section 3 the subband problem with the leading terms of H_{SB}, Eq. 3:

$$H_0 = H_{kin} + U(z) \quad (5)$$

will be solved self-consistently and in Section 4 the influence of H_1 on the subband states is investigated by perturbation theory.

Table 1:

Irreducible tensor components $K_L^{(\kappa,\lambda)*}(\underline{k},\underline{E})$ for zero magnetic field, $\{a,b\}=\frac{1}{2}(ab+ba)$

$K_1^{(1,2)*}$	$\underline{k}^2$
$K_1^{(1,3)*}$	$(\underline{k}^2)^2$
$K_1^{(1,4)*}$	$\{k_x,k_y\}^2 + \{k_y,k_z\}^2 + \{k_z,k_x\}^2$
$K_\alpha^{(4,2)*}$	$\{(k_y^2-k_z^2),k_x\}$, $\{(k_z^2-k_x^2),k_y\}$, $\{(k_x^2-k_y^2),k_z\}$
$K_\alpha^{(6,4)*}$	$(\underline{k}\times\underline{E})_x$, $(\underline{k}\times\underline{E})_y$, $(\underline{k}\times\underline{E})_z$

3. Self-Consistent Calculation

In parabolic approximation the subband problem

$$H_0\psi(\underline{r}) = E\psi(\underline{r}) \quad (6)$$

has been solved before by variational and numerical calculations[1-6]. Eq. 6 can be easily reduced to a one-dimensional Schrödinger equation for the z-direction normal to the interface:

$$H_0(z,k_x,k_y)\xi_i(z) = E_i\xi_i(z) \quad (7)$$

where

Table 2:

Numerical values of the expansion coefficients $a_{K\lambda}$ in Eq. 1. The values in brackets are obtained by neglecting inversion-asymmetry induced terms and coupling to remote bands (see text).

	a_{12}[eVÅ^2]	a_{13}[eVÅ^4]	a_{14}[eVÅ^4]	a_{42}[eVÅ^3]	a_{64}[eVÅ^2]
GaAs	57.29 (57.29)	-2107 (-2311)	-2288 (-1531)	-27.57 (0.0)	5.49 (5.49)
$Ga_{0.75}Al_{0.25}As$	42.49	-1269	-1670	-22.31	2.77
$Ga_{0.7}Al_{0.3}As$	40.11 (40.11)	-1164 (-1287)	-1585 (-911.1)	-22.74 (0.0)	2.45 (2.45)
$Ga_{0.65}Al_{0.35}As$	37.87	-1071	-1508	-21.29	2.23

$$H_0(z,k_x,k_y) = \quad (8)$$
$$-\frac{\hbar^2}{2}\frac{d}{dz}\frac{1}{m^*(z)}\frac{d}{dz} + U(z) + \frac{\hbar^2}{2m^*}k_{||}^2$$

$m^*(z)$ is the bulk mass of GaAs ($Ga_{x-1}Al_xAs$) for $z>0$ ($z<0$). It corresponds to a_{12} in Table 2.

The interface potential is described by:[1-6]

$$U(z) = V_0\,\theta(-z) + V_H(z) + V_{xc}(z) \quad (9)$$

It contains the conduction band discontinuity $V_0\theta(-z)$ and the band bending potential $V_H(z) + V_{xc}(z)$, where $V_H(z)$ is the Hartree potential and $V_{xc}(z)$ a parametrized exchange-correlation potential.[4,19] The magnitude of V_0 depends on the Al concentration in GaAlAs and is taken to be 60% of the band offset.[20,21,22]

The eigenvalue problem (6) is solved self-consistently, using the finite elements method for numerical integration. The boundary conditions at z=0 are determined by flux conservation across the interface.[17,18] As input parameters for the calculation we have the electron concentration N_s, the depletion charge density N_{Depl} and the Al-concentration x in GaAlAs, which takes influence on the effective mass in GaAlAs (see Table 2) and on the conduction band discontinuity V_0.

Calculated subband energies and subband electron densities are consistent with results of previous work.[1-6] They are presented for the lowest two subbands together with the Fermi energy as a function of N_s in Fig. 1. A variation of the Al concentration $0.2 \le x \le 0.4$ shows no significant influence on the above mentioned results.

The average electric field $\langle E_z \rangle$ can be calculated directly as the expectation value of the first derivative of U(z)

$$\langle E_z \rangle = -\frac{1}{e}\int_{-\infty}^{+\infty} \xi_i^2(z)\frac{d}{dz}U(z)dz \quad (10)$$

An alternative derivation is possible using the quantum-mechanical equation of motion, which

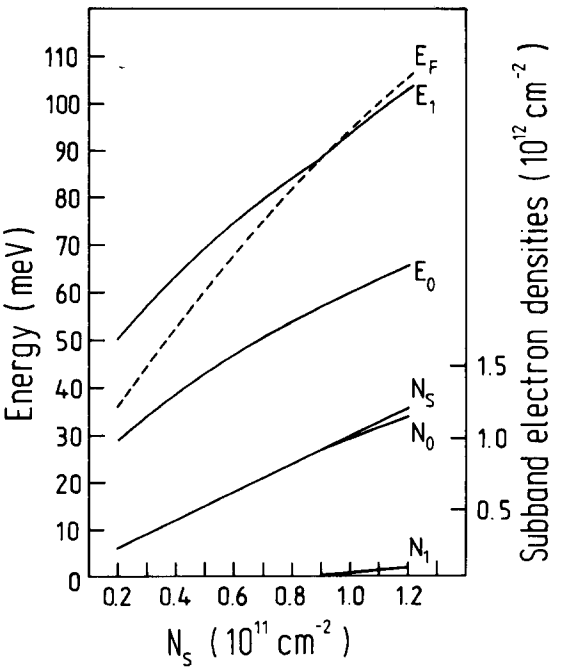

Fig. 1: Calculated subband energies E_0, E_1 and Fermi energy E_F relative to the conduction band minimum at z=0 plotted as function of the subband electron concentration N_s with $N_{Depl}=0.8\times 10^{11}$cm^{-2} and x=0.3, together with corresponding subband electron densities N_0, N_1.

can be used to calculate the average force normal to the interface:

$$\langle F_z \rangle = -\langle [\frac{d}{dz}, H_0] \rangle \quad (11)$$

A simple calculation yields:

$$\langle F_z \rangle = -\frac{\hbar^2}{2}\int_{-\infty}^{+\infty} (\frac{d}{dz}\frac{1}{m^*(z)})(\frac{d}{dz}\xi_i(z))^2 dz$$

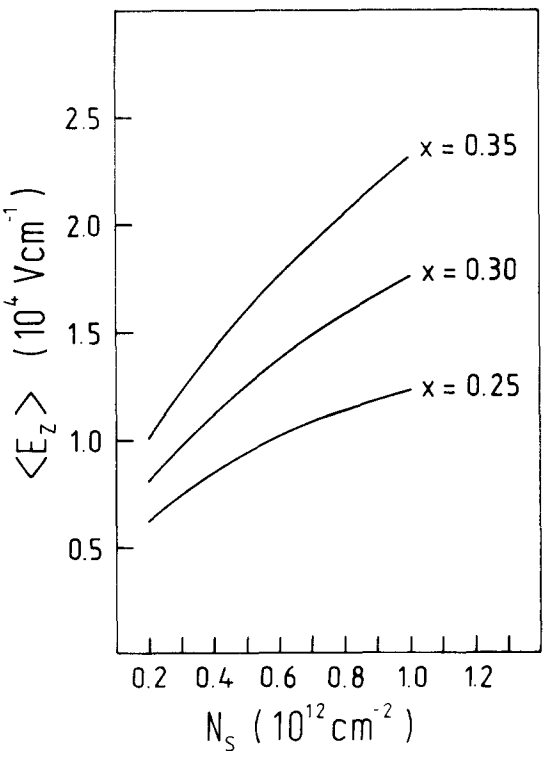

Fig. 2: Calculated values of the average electric field $\langle E_z \rangle$ as a function of the subband electron concentration N_S at $N_{Depl}=0.8\times10^{11}cm^{-2}$ and x=0.25, 0.30, 0.35.

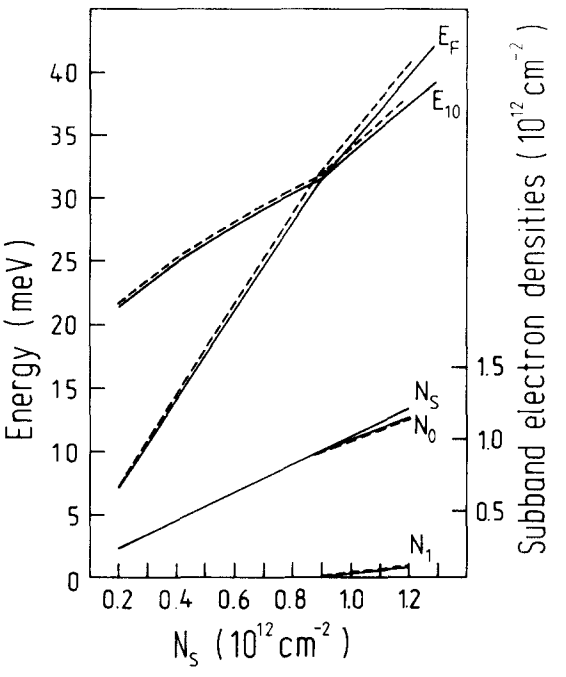

Fig. 3: Calculated subband separation E_{10}, Fermi energy E_F and subband occupation N_0, N_1 as function of the electron concentration N_S with $N_{Depl}=0.8\times10^{11}cm^{-2}$ and x=0.3. Solid (dashed) curves correspond to calculations with (without) nonparabolic corrections to the density of states.

$$-\int_{-\infty}^{+\infty} \xi_i^2(z)\left(\frac{d}{dz}U(z)\right)dz \qquad (12)$$

The quantum mechanical statement, that particles in bound states cannot be subject to a finite force, i.e. $\langle F_z \rangle=0$, has been verified within the limit of numerical precision by calculating the integrals of Eq. 12 using the self-consistent solutions of the subband problem. This result demonstrates that there is a nonvanishing average electric field for subband states, whenever the effective mass is position dependent. This statement is true also for subband states in MIS structures, for which the effective mass changes from the bulk value of the semiconductor to a value close to the free electron mass in the insulator. This fact has not been considered in Ref. 13.

Calculated results for the average electric field in a GaAs/$Ga_{x-1}Al_xAs$ are shown in Fig. 2 for electron concentrations $10^{11}cm^{-2}\leq N_S\leq10^{12}cm^{-2}$ at three different Al-concentrations x.

4. Influence of Nonparabolic Corrections

Starting from the self-consistent solutions of Section 3 we can now consider the nonparabolic correction $H_1(\underline{k},\underline{E})$. This is done by a perturbation calculation using the spinor wave function

$$\chi_i(z) = c_\uparrow\binom{1}{0}\xi_i(z) + c_\downarrow\binom{0}{1}\xi_i(z) \qquad (13)$$

and minimizing the expectation value of the total Hamiltonian H (Eq. 1) by variation with respect to $c_\uparrow$, $c_\downarrow$. At the same time the change in the density of states due to the nonparabolic corrections is considered in the self-consistent solution of Section 3. Warping effects are neglected by averaging in the plane parallel to the interface.

Fig. 3 shows the effect of the change in the density of states on the subband separation E_{10}, Fermi energy E_F, and subband occupation. It can be seen, that due to nonparabolicity the occupation of the second subband starts at higher N_S. The variational calculation for the expectation value of the subband Hamiltonian yields a dispersion relation:

$$E_i(k_{||}) = E_i + E_{ip}(k_{||}) \pm E_{is}(k_{||}) \qquad (14)$$

for each subband i. E_i is the i^{th} subband energy at $k_{||}=0$.

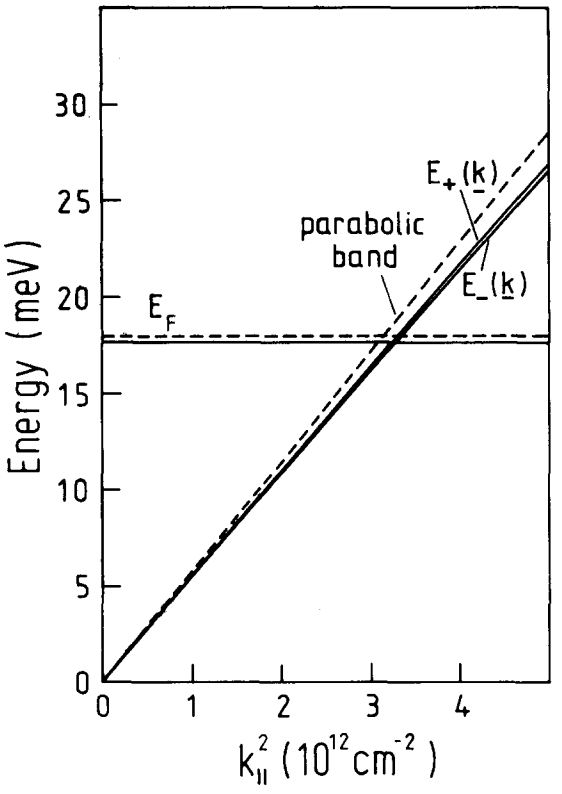

Fig. 4: Subband dispersion as a function of $k_{||}^2$ for $N_s=5\times10^{11}cm^{-2}$, $N_{Depl}=0.8\times10^{11}cm^{-2}$ and x=0.3. The dashed curve corresponds to the simple parabolic case.

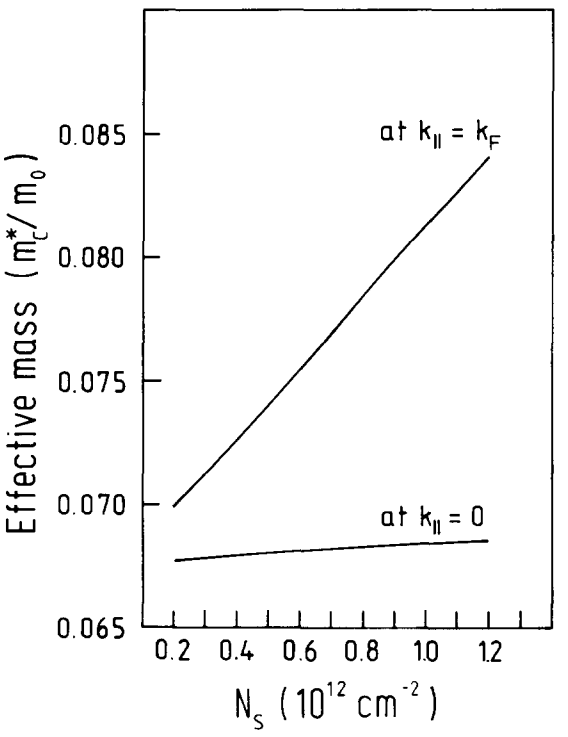

Fig. 5: Effective mass of GaAs as a function of N_s ($N_{Depl}=0.8\times10^{11}cm^{-2}$, x=0.3) at $k_{||}=0$ and at $k_{||}=k_F$.

$$E_{ip}(k_{||}) = \frac{\hbar^2}{2m^*}k_{||}^2 - \langle\frac{d}{dz}(2a_{13}+a_{14})\frac{d}{dz}\rangle k_{||}^2 + (a_{13}+\frac{1}{8}a_{14})k_{||}^4 + \langle\frac{d^2}{dz^2}a_{13}\frac{d^2}{dz^2}\rangle \quad (15)$$

describes the subband dispersion without spin-splitting. The corrected effective mass is defined by

$$\frac{1}{m_c^*} = \frac{1}{m^*} - \frac{2}{\hbar^2}\langle\frac{d}{dz}(2a_{13}+a_{14})\frac{d}{dz}\rangle + \frac{12}{\hbar^2}(a_{13}+\frac{1}{8}a_{14})k_{||}^2 \quad (16)$$

The spin-splitting

$$E_{is}(k_{||}) = (\Delta_{42}+\Delta_{SO})^{1/2} \quad (17)$$

results from the $\underline{k}^3$-nonparabolicity

$$\Delta_{42} = -\frac{1}{8}k_{||}^4\langle a_{42}\frac{d}{dz} + \frac{d}{dz}a_{42}\rangle^2 + \frac{1}{2}a_{42}k_{||}^4\langle\frac{d}{dz}a_{42}\frac{d}{dz}\rangle + k_{||}^2\langle\frac{d}{dz}a_{42}\frac{d}{dz}\rangle^2 + \frac{1}{8}a_{42}^2k_{||}^6 \quad (18)$$

and the spin-orbit term

$$\Delta_{SO} = a_{64}^2k_{||}^2\langle E_z\rangle^2 \quad (19)$$

Fig. 4 shows the subband dispersion $E_i(k_{||})$ of Eq. 15 for $N_s=5\times10^{11}cm^{-2}$, which exhibits a deviation from the parabolic form and a lifting of the spin degeneracy. The effective mass at $k_{||}=0$ and $k_{||}=k_F$ for fixed N_{Depl},x and an electron concentration $10^{11}cm^{-2}\leq N_s\leq1.2\times10^{12}cm^{-2}$ is plotted in Fig. 5. It is not possible to compare these results for the dispersion effective mass with cyclotron masses from cyclotron experiments,[23,24,25] but the values at $k_{||}=0$ and $k_{||}=k_F$ can be taken as bounds for the measured cyclotron masses.

The spin-splittings for $10^{11}cm^{-2}\leq N_s\leq1.2\times10^{12}cm^{-2}$ at fixed N_{Depl},x is shown in Fig. 6. It turns out that the influence of the spin-orbit coupling is small for a GaAs/$Ga_{x-1}Al_xAs$ heterostructure and the main contribution is due to the inversion asymmetry-induced $\underline{k}^3$ nonparabolicity.

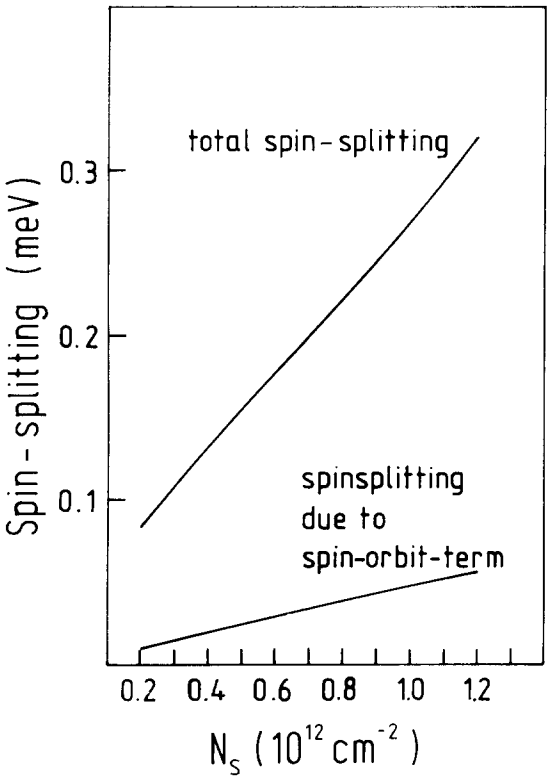

Fig. 6: Total spin-splitting energy and spin-splitting energy at $k_{\parallel}=k_F$ due to spin-orbit-interaction as a function of N_S ($N_{Depl}=0.8\times10^{11}cm^{-2}$, x=0.3).

5. Conclusion

Using a self-consistent solution of the subband problem in parabolic approximation we consider the influence of the nonparabolicity of the bulk band structure on the electron states in GaAs/$Ga_{1-x}Al_xAs$ heterostructures. Our main results: change of the density of states, shift of the subband energies, increase of the effective mass and spin-splitting of the subband at finite $k_{\parallel}$, demonstrate the importance of the nonparabolic effects for a quantitative understanding of the 2-dimensional electron system.

For a comparison with experimental data (cyclotron and electron spin resonance) it is necessary to take into account the magnetic field, which is done in the following paper.

References

1. T. Ando, J. Phys. Soc. Jpn. 51, 3893 (1982)
2. T. Ando, J. Phys. Soc. Jpn. 51, 3900 (1982)
3. G. Bastard, Surf. Sci. 142, 284 (1984)
4. F. Stern, S. DasSarma, Phys. Rev. B 30, 840 (1984)
5. G.A.M. Hurkx, W. van Haeringen, J. Phys. C 18, 5617 (1985)
6. T. Ando, A.B. Fowler, F. Stern, Rev. Mod. Phys. 54, 437 (1982)
7. E.O. Kane, J. Phys. Chem. Solids 1, 249 (1957)
8. U. Rössler, Solid State Commun. 49, 943 (1984)
9. R. Lassnig, Phys. Rev. B 31, 8076 (1985)
10. F.J. Ohkawa, Y. Uemura, J. Phys. Soc. Jpn. 37, 1325 (1974)
11. M. Braun, U. Rössler, J. Phys. C 18, 3365 (1985)
12. Y.A. Bychkov, E.I. Rashba, J. Phys. C 17, 6039 (1984)
13. A. Därr, J.P. Kotthaus, T. Ando, Proc. of the 13th Int. Conf. Physics Semiconductors, Rome 1976, p. 774
14. G. Lommer, F. Malcher, U. Rössler, Phys. Rev. B 32, 6965 (1985)
15. G.L. Bir, G.E. Pikus, Symmetry and strain induced effects in semiconductors, New York: Wiley § 25,26 (1974)
16. Landolt-Börnstein, Series III, Vol. 17a: Semiconductors, ed. O. Madelung, Springer New York (1982)
17. R.A. Morrow, K.R. Brownstein, Phys. Rev. B 30, 678 (1984)
18. D.J. BenDaniel, C.B. Duke, Phys. Rev. 152, 683 (1966)
19. L. Hedin, B.I. Lundqvist, J. Phys. C 4, 2064 (1971)
20. R.C. Miller, D.A. Kleinmann, A.C. Gossard, Phys. Rev. B 29, 7085 (1984)
21. D.C. Rogers, R.J. Nicholos, J. Phys. C 27, 891 (1985)
22. H. Hihara, C. Hamaguchi, Solid State Commun. 54, 485 (1985)
23. H. Sigg, P. Wyder, J.A.A.J. Perenboom, Phys. Rev. B 31, 5253 (1985)
24. K. Muro et al., Surf. Sci. 113, 321 (1982)
25. H.L. Störmer et al., Solid State Commun. 29, 705 (1979)